Research Paper

Design and Characterization of Fosfestrol Cubosomes for Effective Management of Prostate Cancer

S. S. HARALE, A. G. PATIL[1], S. T. GALATAGE[2]*, A. S. MANJAPPA[2], P. S. KUMBAHR[3], K. S. MIRAJKAR[4] AND S. G. KILLEDAR[5]

Department of Pharmacy, Sant Gajanan Maharaj College of Pharmacy, [1]Sant Gajanan Maharaj Rural Hospital and Research Center, Mahagoan 416502, [2]Vasantidevi Patil Institute of Pharmacy, [3]Tatyasaheb Kore College of Pharmacy, Kolhapur, Maharashtra 416114, [4]Department of Pharmaceutics, KLEs College of Pharmacy, Nippani, Karnataka 591237, [5]Anandi Pharmacy College, Kolhapur, Maharashtra 416205, India India

Prostate carcinoma is the second most leading cause of tumor deaths worldwide and incidence has increasing significantly. In spite of dominant efficacy fosfestrol in treatment of prostate cancer it has hurdles like poor water solubility, low bioavailability and potential side effects on oral administration. The advanced drug delivery approach, cubosomes are reported to show improved oral solubility and bioavailability, and improved anticancer activity. Therefore, the present research was aimed to develop fosfestrol cubosomes to improve solubility, and anticancer efficacy against prostate cancer. Cubosomes were developed by using solvent evaporation technique and optimized using 3^2 factorial design to verify effect vesicle size and entrapment efficiency using poloxamer-407 as emulsifier and glyceryl monooleate as lipid. The optimized fosfestrol cubosomes were lyophilized using freeze dryer and characterized for morphology by transmission electron microscope, crystallinity by X-ray diffraction, drug release, cytotoxicity, apoptotic potential etc. Optimized fosfestrol cubosomes displayed a mean vesicle size of (183.6±3) nm with polydispersity index 0.248±0.030, zeta potential of -24.6±2.54 mV. Moreover, the percent entrapment efficiency of cubosomes was found to be 94.48 %±4.54 %. Lyophilized fosfestrol cubosomes appeared as unilamellar nano vesicles with somewhat round cubic shapes which displayed maximum release of fosfestrol 93.48 %±3.64 % after 3 h in 0.1 N hydrochloric acid. The fosfestrol cubosomes demonstrated significantly ($p<0.01$) higher *in vitro* cytotoxic (low half-maximal inhibitory concentration value (8.30±0.62) µg/ml than plain fosfestrol (22.37±1.82) µg/ml. In addition, flow cytometry results revealed that large proportion of cells were entered in apoptotic stage compared to control and negative control revealing remarkable apoptotic potential of fosfestrol cubosomes. The obtained results revealed the momentous anticancer activity of fosfestrol delivered *via* cubosomes. Therefore, the developed fosfestrol cubosomes can be used as competent alternative to systemic chemotherapy in effective management of prostate cancer. However, further *in vivo* animal studies are required to establish its efficacy in the treatment of prostate cancer.

Key words: Prostate cancer, fosfestrol, poloxamer-407, cubosomes, optimization, cytotoxicity, apoptosis

Cancer is a chief health concerns and leading cause of mortality worldwide. Cancer is abnormal growth cells which infiltrate normal cells and tissues rapidly grow in any part of body and may infect other organs. Different type of cancer may affect various body parts or area such as kidney, blood, liver, lung, and breast[1]. Prostate cancer is 2nd leading cause of deaths in men. Chemotherapy is a primarily used treatment modalities against kinds of cancers. Fosfestrol (FST) known as diethylstilbestrol which is principally employed in the treatment of prostate cancer. However, it is allied with various drawbacks such as poor water solubility, dose-related adverse effects and lack of selectivity towards cancer cells[2]. Therefore, to overcome the aforementioned shortcomings in the delivery of FST, Advanced Drug Delivery Systems (ADDS) plays an imperative role.

***Address for correspondence**
E-mail: gsunil201288@gmail.com

Accepted 25 October 2024
Revised 27 May 2024
Received 30 September 2022
Indian J Pharm Sci 2024;86(5):1734-1746

ADDS including cubosomes, liposomes, niosomes, transferosomes, and colloidosomes have shown promise in the delivery of anticancer therapeutics against variety of cancers. Cubosomes are the nanostructured particles which are self-assembled and having large internal surface area and cubic crystalline structure. The cubic phase of cubosomes can be fractured and dispersed that result in the formation of the particulate dispersion which is thermodynamically stable for long period of time[3,4]. Cubosomes provide a platform for adjusting the lipids and stabilizers to obtain a carrier with the desired characteristics for targeted drug delivery. The different types of benefits offered by cubosomes include ability to load hydrophilic and hydrophobic therapeutics, high drug loading capacity, improved stability and bioavailability, targeted delivery, and non-toxicity. For instance, Fahmy *et al*.[5] have successfully fabricated icariin-loaded cubosomes with improved solubility and bioavailability in the effective treatment of ovarian cancer. They found substantial improvement in the solubility and bioavailability of icariin when delivered[6,7].

In another study, Nasr *et al*.[8] have developed cubosomes for liver cancer targeted delivery of 5-Fluorouracil (5-FU). The cubosomes have displayed 5-folds augmented in the concentration of 5-FU when compared to the plain 5-FU. Furthermore, cubosomes have been reported to target cancer cells by both active and passive targeting pathway because of their very small size that cause easy passage of cubosomes to the tight junction of endothelial cells[4]. Therefore, the chief objective of the current research was to develop, optimize and characterize FST cubosomes for effective treatment of prostate cancer.

MATERIALS AND METHODS

FST kindly gifted by Cadila Healthcare Pvt. Ltd., Glyceryl Monooleate (GMO) supplied by Mohini Organics Pvt. Ltd., Mumbai, India, P-407 kindly gifted by Badische Anilin and Sodafabrik (BASF) Mumbai, India. Chloroform, ethanol and methanol procured from Loba Chemie Ptv. Ltd., Mumbai, India. All other chemicals used in current research work were of analytical grade. Cell culture the sensitive prostate cancer cells (Lymph Node Carcinoma of the Prostate (LNCaP) were procured from National Center for Biotechnology Information (NCBI), Pune, India.

Compatibility studies:

Fourier Transforms Infrared (FTIR) spectroscopy: FTIR of plain FST, plain Poloxamer-407 (P-407), GMO, and FST with formulation excipients of cubosomes (physical mixture; in 1:1 weight ratio) was carried out to evaluate FST and excipients compatibility using a Bruker, Alpha-T over the wave number of 4000 to 650 cm-1[6].

Differential Scanning Colorimetry (DSC): DSC of plain FST, plain P-407, GMO, and FST with cubosomes formulation excipients (1:1 weight ratio) was performed to judge the compatibility of FST-excipients and any changes in the physical state of FST on entrapment in cubosomes by DSC (DSC-60, Shimadzu, Japan)[7].

Preparation and optimization of FST-loaded cubosomes: The cubosomes formulation was prepared and optimized by employing 3^2 factorial designs with Design-Expert® software (Version 12.0, Stat-Ease Inc., United States of America (USA)). Nine diverse formulations as insinuated by design at three different coded levels (-1, 0 and +1) of concentration of GMO (X1) and P-407 (X2) were designed (Table 1). The batches were optimized based on vesicle size (Y1) and Percent Entrapment Efficiency (% EE) (Y2). Briefly, FST-loaded cubosomes were prepared by dissolving GMO and P-407 in 15 ml of chloroform, and then allowed to evaporate under reduced pressure (at 60 revolutions per minute (rpm) and 60°±2°) using rotary evaporator (Buchi R-300) leading to formation of thin film. A solution of FST (120 mg) in methanol (50 ml) was added to dry lipid film to form coarse dispersion. The dispersion was sonicated and reserved under hot water (80°±2°) for 15 min in water bath and then homogenized using high speed homogenizer (IKA T-25) for 1 min at 13 500 rpm to obtain uniform dispersion. Finally, the dispersion was cooled resulting formation of cubosomes[8,9].

TABLE 1: 3^2 FULL FACTORIAL DESIGN FOR FST LOADED CUBOSOMES

Standard	Run	Factor 1	Factor 2	Response 1	Polydispersity Index (PDI)	Response 2
		GMO (mg)	P-407 (mg)	Vesicle size (nm)		EE %
7	1	360	150	183.6±3	0.248±0.030	92.54±2.67
9	2	360	100	152.3±2	0.258±0.026	90.22±2.94
8	3	360	50	184.2±4	0.247±0.031	78.54±4.21

4	4	540	150	390.8±6	0.324±0.025	94.12±3.75
3	5	180	150	117.6±2	0.210±0.036	86.72±3.64
6	6	540	100	278.3±3	0.256±0.025	91.86±3.35
2	7	540	50	306.6±5	0.378±0.023	96.34±2.43
5	8	180	100	148.3±2	0.217±0.020	76.72±3.85
1	9	180	50	138.7±3	0.246±0.029	68.22±5.41

NOTE: *values are mean±SD (N=3)

Characterization of FST-loaded cubosomes:

Vesicle size and Zeta Potential (ZP): The mean vesicle size of all the formulated batches of cubosomes, and ZP of optimized batch was determined by Zetasizer (Nano ZS, Malvern, United Kingdom (UK)). 1 ml sample of each formulation was diluted with deionized water (29 ml) and analyzed in triplicate at 25°±0.5°[10].

% EE: Briefly, the cubosomes were alienated from the aqueous medium by centrifugation (10 000 rpm for 1 h). Then, the amount of free FST in the buoyant was estimated by Ultraviolet (UV) spectrophotometry at 243 nm after suitable dilution with methanol[11]. The FST entrapped in the cubosomes was calculate using formula,

% EE =Tp-Tf/Tp×100

Where, Tp is the total FST used to prepare the cubosomes and Tf is the free FST in the supernatant.

Freeze drying and characterization of lyophilized cubosomes powder: The optimized cubosomes and trehalose cryoprotectant (at varying weight ratios) were lyophilized *via* Martin Christ (Alpha 1-2 LDplus) freeze dryer. The lyophilized powders were then subjected for diverse characterization.

Process yield of freeze drying process: The quantity of product achieved after completion of process is determined by process yield. Briefly, powder obtained after lyophilization (Martin Christ lyophilize) was collected and product yield was calculated from following equation[12].

% process yield=practical yield/theoretical yield×100

Surface morphology:

Surface morphology of lyophilized powder of FST-cubosomes was studied by using Transmission Electron Microscopy (TEM). Briefly, the lyophilized cubosomes suspension (reconstituted with Water for Injection (WFI)) was located on a carbon coated copper grid and permitted to fix and air dried. Finally, sample was stained with 1 % uranyl acetate (negative stain) for 3-5 min and observed using TEM (JEOL-USA, Wilmington, Delaware, USA)[13].

Powder X-Ray Diffraction (P-XRD):

The crystallinity of FST and lyophilized cubosomes was assessed using P-XRD ((Philips-diffractometer, The Netherlands) operated at 40 kV, at 30 mA. The samples were scanned from 4-600 with an augmentation of 0.020 and diffraction angle (2θ) at 1 s/step at a room temperature[14].

***In vitro* release study:**

In vitro dissolution of optimized lyophilized FST cubosomes was carried out using dissolution test apparatus United States Pharmacopeia (USP) type-I (Basket type). Lyophilized FST cubosomes were filled in to size '0' capsule and kept in dissolution test apparatus containing 900 ml of 0.1 N Hydrochloric acid (HCl) at 37°±2° and 50 rpm. The 1 ml of sample was withdrawn at predetermined interval of time and same volume was substituted with fresh dissolution fluid. Finally, the samples were assayed by UV-spectrophotometer at 243 nm[15,16].

Cytotoxicity study:

The outcome of plain FST and optimized lyophilized cubosomes on viability of LNCaP cells was studied by using 3-(4,5-Dimethylthiazol-2-yl)-2,5-Diphenyltetrazolium Bromide (MTT) dye reduction assay. Briefly, cells were added to a 96-well plate and overnight incubated at 37°. At specific concentrations (100, 50, 25, 12.5, 6.25 and 3.125) µg/ml cells were treated with samples and plates were incubated for another 48 h. Then 100 µl of MTT (6 mg/10 ml of MTT in Phosphate-Buffered Saline (PBS)) was added in the plates by removing test solutions and plates were further incubated for 4 h in an analogous environment. Finally, the buoyant was discarded and formazan crystals produced in viable cells were solubilized by Dimethyl Sulfoxide (DMSO) (100 µl). The absorbance of the ensuing solution was deliberated at 570 nm using a microplate. The half-maximal Inhibitory Concentration

(IC_{50}) values were then calculated using dose-response curves[17].

Apoptosis by flow cytometer:

The cells were preserved overnight by placing in a 24-well micro plate at 37°. The cells were then incubated with 50 µg/ml of plain FST and optimized lyophilized cubosomes for 24 h. Following incubation, cells were centrifuged for 5 min at 4° and cell pellet was collected. The ensuing pellets were washed repeatedly using a 2 ml of 1×PBS and supernatant was discarded. Then 1 µl of annexin-V solution and 5 µl Propidium Iodide (PI) was added and tubes were kept on ice. Finally, the 400 µl of ice-cold buffer was added into the tubes incubated in dark for 15 min and were analyzed by flow cytometry within 30 min[18,19].

Apoptosis by 4,6-Diamidino-2-Phenylindole (DAPI) staining:

Briefly, 1×10^4 cells/well were introduced in a 24-well plate and reserved overnight in Carbon dioxide (CO_2) incubator at 37° and were treated with compounds (<50 µg/ml) and incubated for 24 h. The cells were then washed using PBS and fixed with paraformaldehyde (4 %) for 30 min and incubated with 20 µl of DAPI (0.1 µg/ml) in a dark and evaluated. The cells undergone apoptosis were counted by randomly selecting the microscopic fields and the % of apoptotic cells were calculated[20].

Stability study:

Stability study of lyophilized FST cubosomes was carried out at 40°±2° and 75 %±5 % Relative Humidity (RH) for 90 d (as per International Conference on Harmonization (ICH) guidelines) and its physical stability was estimated by evaluating parameters like drug content, % drug release after specific time intervals (1, 2 and 3 mo).

RESULTS AND DISCUSSION

FTIR was performed to ascertain compatibility between the FST and excipients of cubosomes. The FTIR spectra of pure FST, P-407 and GMO, FST and formulation excipients of cubosomes are shown in fig. 1. In the FTIR spectra of FST (fig. 1A), the peaks at 2863.46 cm^{-1}, 1650.16 cm^{-1} and 3345.17 cm^{-1} are attributed to the characteristic peaks of C-H, C=C, and aromatic C-H stretching of FST. Besides, the peak at 1501.66 cm^{-1} is a characteristic peak of $O\text{-}PO_3$ functional group of FST. The FTIR spectra of P-407 (fig. 1B), showed a peak at 2891.39 cm^{-1} which is a peak of carboxylic acid aliphatic stretch. Moreover, the peak at 1112.96 cm^{-1} , 3433.41 cm^{-1}, 1467.88 cm^{-1} and 1637.62 cm^{-1} are characteristic peaks attributed to the C-O-C (ether) dialkylstretch, O-H stretch, C-H stretch, and O-H stretch of P-407 respectively. In the FTIR spectra of GMO (fig. 1C), the peaks at 3007.12 cm^{-1}, 2924.18 cm^{-1}, 1741.78 cm^{-1} and 1246.6 cm^{-1} are the peaks of CH stretch, CH stretching (carbonyl), C=O stretching and C-O stretching of GMO respectively. The FTIR spectra of FST and cubosomes excipients (fig. 1D) displayed a peak at 2863.62 cm^{-1} which is a characteristic peak of C-H stretch, peak at 1642.87 cm^{-1} and 3347.67 cm^{-1} are attributed to the C=C and C-H aromatic stretching of FST. The results revealed that the fundamental peaks of the FST are retained in the physical mixture of FST and cubosomes excipients indicating no interaction (compatibility) between FST and cubosome excipients used[21,22].

DSC of FST, GMO, P-407 , and FST and formulation excipients of cubosomes are depicted in fig. 2. In the DSC thermogram of FST, GMO and P-407, sharp endothermic melting peak was observed at 256° (fig. 2A), 32° (fig. 2B) and 63° (fig. 2C) which is attributed to the peak of FST, GMO and P-407, respectively. However, in the DSC thermogram of FST with cubosomes excipients (fig. 2D), no characteristic endothermic peak related to the FST was observed while endothermic melting peaks at 40° and 61° were observed which may be corresponds to GMO and P-407 respectively. These results indicate that FST may be molecularly dispersed in cubosomes dispersion. Furthermore, the amorphous state of FST in the cubosomes revealed the complete entrapment of FST inside the lipid matrix of the cubosomes[22,23].

Contour plot fig. 3A and fig. 3B, surface response plot (fig. 3B) were used to divulge the consequence of GMO (A) and P-407 (B) on vesicle size. The increase in the percentage of a caused an augment in the vesicle size of cubosomes. In contrast, an augment in B caused decrease in the vesicle size of cubosomes. The mean particle size of all batches of FST-cubosomes was observed in the range of 117.6-390.8 nm as shown in Table 1 and PDI in the range of 0.210 to 0.378. The batch F5 displayed smallest vesicle size (117.6 nm) (fig. 4A) when compared to other batches. The Analysis of Variance (ANOVA) analysis of results yielded F-value 12.73 and p-value 0.0311, which indicates the implication of the quadratic model (Table 2). The relevant model for vesicle size (R^2=0.999) was observed to be a quadratic model final equation in terms of coded factors polynomial equation for vesicle size

is, vesicle size, $Y1=155.18i+95.18A+10.42B+26.32AB+56.68A^2+27.28B^2$

Contour plot (fig. 4A and fig. 4B) surface response plot (fig. 4B) was used to reveal the outcome of GMO (A) and P-407 (B) on % EE. Both A and B elicited the positive effect (increase in the A and B caused augment in the EE) on EE. Besides, a decrease in the EE was observed with the interaction amid two variables. The maximum EE was obtained for FST-cubosomes-7 (96.34 %), while the minimum value was attained for FST-cubosomes-9 (68.22 %). The ANOVA analysis of results yielded F-value 12.24 and p-value 0.0329, which indicates the implication of the quadratic model (Table 3). The relevant model for drug content ($R^2=0.996$) was observed to be a quadratic model. Final equation in terms of coded factors or polynomial equation for EE is, $\%\ EE=87.22i+8.44A+5.05B-5.18AB-1.44A^2-0.1867B^2$

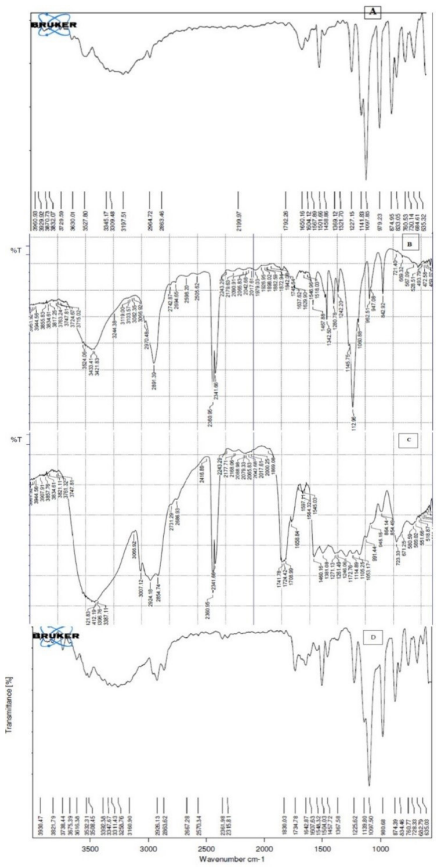

Fig. 1: FTIR, (A): FST; (B): GMO; (C): P-407 and (D): FST cubosomes

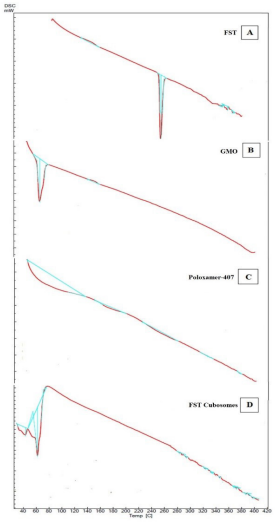

Fig. 2: DSC, (A): FST; (B): GMO; (C): P-407 and (D): FST cubosomes

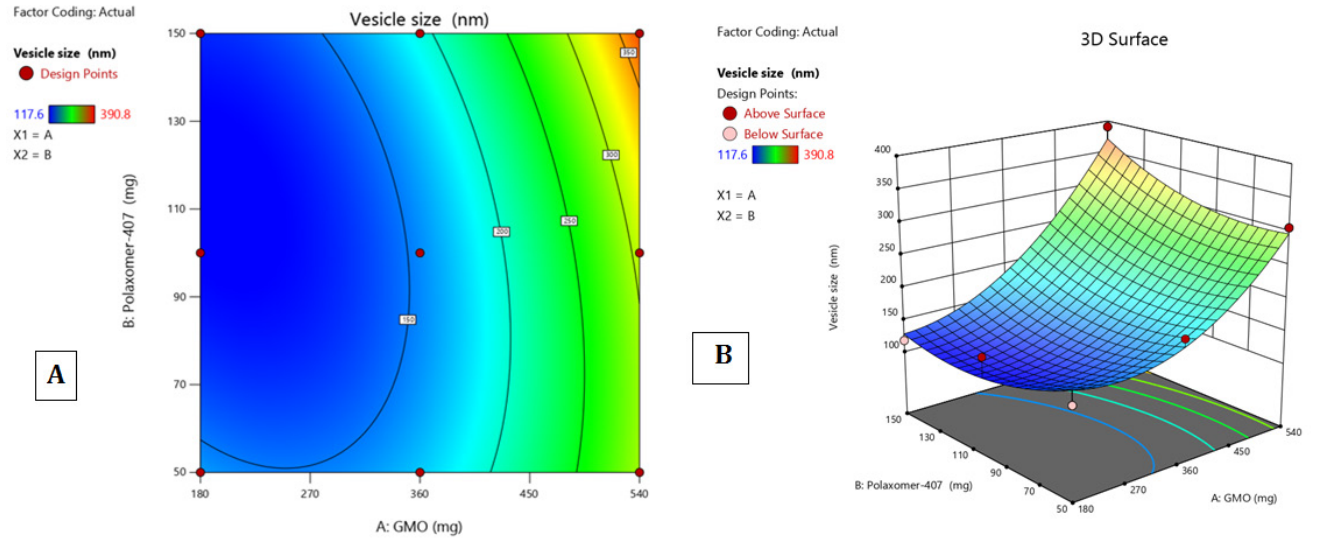

Fig. 3: (A): Contour plots (2D) showing the effect of GMO (X1) and P-407 (X2) on vesicle size (Y1) and (B): Response surface plots (3D) showing the effect of GMO (X1) and P-407 (X2) on vesicle size (Y1)

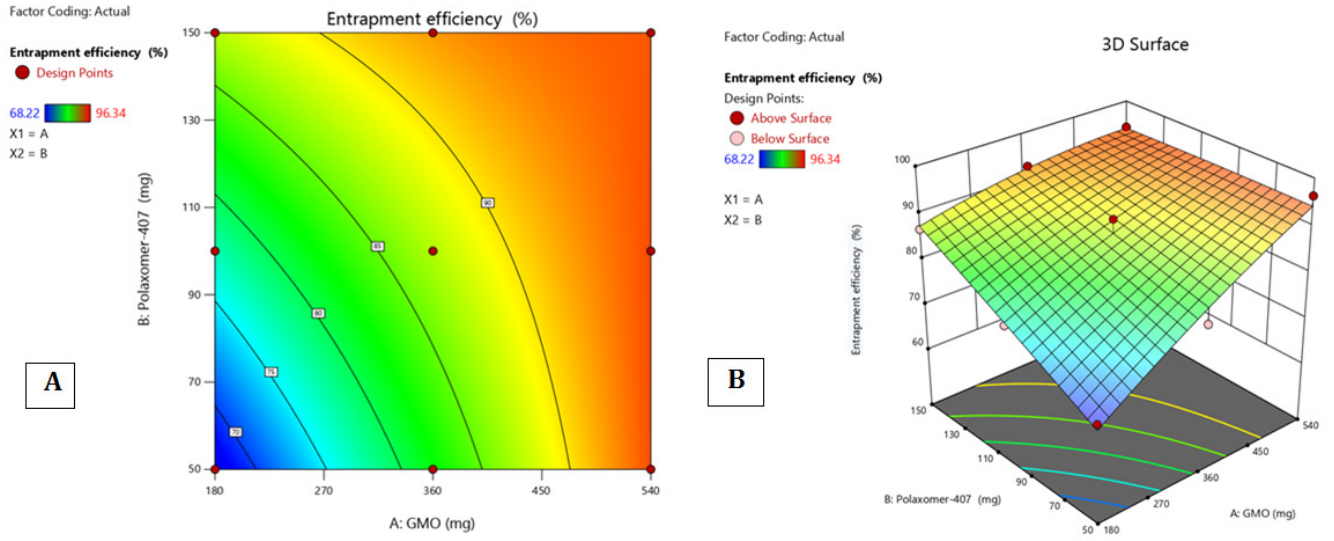

Fig. 4: (A): Contour plots (2D) showing the effect of GMO (X1) and P-407 (X2) on % EE (Y2) and (B): Response surface plots (3D) showing the effect of GMO (X1) and P-407 (X2) on % EE (Y2)

TABLE 2: ANOVA FOR VESICLE SIZE (Y1)

Source	Sum of squares	Degrees of freedom (df)	Mean square	F-value	p-value
Model	65697.03	5	13139.4	12.73	0.0311
GMO	54359.20	1	54359.20	52.67	0.0054
P-407	651.04	1	651.04	0.6308	0.4851
AB	2772.02	1	2772.02	2.69	0.1998
A^2	6426.00	1	6426.00	6.23	0.0881
B^2	1488.76	1	1488.76	1.44	0.3159
Residual	3096.28	3	1032.09		
Corrected total	68793.30	8			

TABLE 3: ANOVA FOR % EE (Y2)

Source	Sum of squares	df	Mean square	F-value	p-value
Model	692.08	5	138.42	12.24	0.0329
GMO	427.74	1	427.74	37.83	0.0086
P-407	152.81	1	152.81	13.51	0.0349
AB	107.33	1	107.33	9.49	0.0541
A^2	4.13	1	4.13	0.3650	0.5883
B^2	0.0697	1	0.0697	0.0062	0.9424
Residual	33.92	3	11.31		
Corrected total	726.00	8			

Among the 9 batches prepared, batch F1 displayed vesicle size (183.6±3 nm) (fig. 5A) and PDI of 0.248±0.030 and substantially higher % EE 92.54±2.67 when compared to other batches. Therefore, batch F1 was considered as optimized batch and used for further characterization. The formulation and optimization of 9 batches of colloidosomes is depicted in (Table 1).

ZP denotes stability of nano-vesicular systems and dispersions. The ZP of the optimized FST cubosomes was observed to be -24.6±0.4 mV (fig. 5B) which is indication of good stability of developed FST cubosomes. A high ZP value is indicator of long-term stability developed formulation which avoids aggregation[24,25].

The optimized cubosomes (F1) was lyophilized using a cryoprotectant trehalose to keep formulation physically and chemically stable till further characterization. This lyophilized formulation displayed % process yield of 91.57 %±3.25 % at optimized parameters (primary and final drying for 6 h at -50° and 0.05 mbar).

Surface morphology of the FST-cubosomes was investigated by TEM. In the TEM analysis, cubosomes appeared as unilamellar vesicles which are smooth and cubic shape and in nanometer size range (fig. 6).

X-ray diffractometer of plain FST exhibited characteristic intensity reflections counts of 2344, 2220, 1170 and 1394 at diffraction angles of 15.100, 15.980, 25.355 and 29.856 (2θ), respectively, (fig. 7A) implicating its crystalline nature. However, these characteristic peaks were disappeared in the XRD pattern of FST-loaded cubosomes (fig. 7B-fig. 7D).

Drug release profile of optimized lyophilized FST cubosomes and plain FST in 0.1 N HCl is shown in fig. 8. The FST cubosomes showed significantly higher % release (93.48 %±3.64 %) of FST as compared to pure FST (48.51 %±2.72 %).

The *in vitro* cytotoxicity of lyophilized FST cubosomes was studied against LNCaP cells using MTT assay and compared with plain FST. The % viability LNCaP cells with respect to formulation concentration after 48 h incubation was depicted in fig. 9. The lyophilized cubosomes exhibited significant ($p<0.01$) cytotoxicity (low IC_{50}: 8.30±0.62 µg/ml) than plain FST (22.37±1.82 µg/ml) against LNCaP cells respectively after 48 h of incubation.

The cytometric evaluation of LNCaP cells treated with plain FST and lyophilized FST cubosomes was shown in fig. 10. In control sample, the untreated cells are predominantly healthy (100 % live cells) with only 0.01%, 0.01 %, and 0.031 % of the cells were in early, late apoptotic and necrotic states (fig. 10A). About 7.55 % of the cells were found in early apoptotic state and 16.9 % of the cells were observed in late apoptotic stage treated with FST. Thus, the % of live cells rapidly decreased from 100 % to 69.5 % when treated with FST (fig. 10B). In contrast, the cells treated with optimized lyophilized cubosomes, only 16.6 % and 14.9 % of the cells were found in early and late apoptotic state respectively. Thus, the % of live cells drastically reduced from 99.70 % to 57.9 % when treated with optimized lyophilized FST cubosomes (fig. 10C).

DAPI staining technique was utilized to check programmed cell death for 48 h in LNCaP prostate cancer cells after treatment with FST and lyophilized FST cubosomes. Nuclear morphological changes in negative control cells, FST treated lyophilized FST cubosomes treated cells are shown in fig. 11. Negative control (untreated cells) (fig. 11A) showed weak homogenous blue staining along with intact

normal nuclei whereas, in the cells treated with FST (fig. 11B) and lyophilized FST cubosomes (fig. 11C), circle represents chromatin condensation and nuclear shrinkage, square represents nuclear blabbing, nuclear fragmentation and arrow represents apoptotic bodies. The percentage apoptosis for control, plain FST and lyophilized FST cubosomes was found to be 2.62±1.46, 51.52±4.12 and 68.12±5.85, respectively.

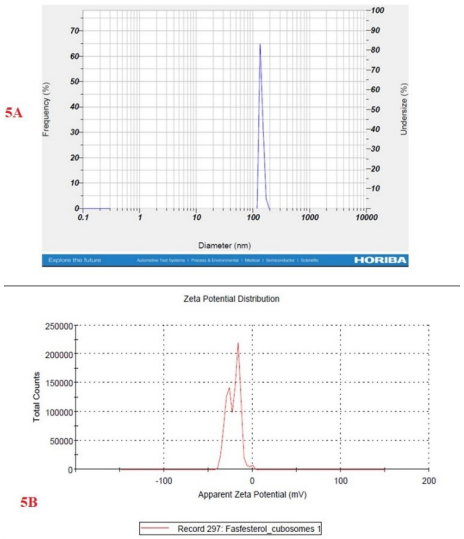

Fig. 5: (A): Particle size distribution and (B): ZP of FST cubosomes optimized batch

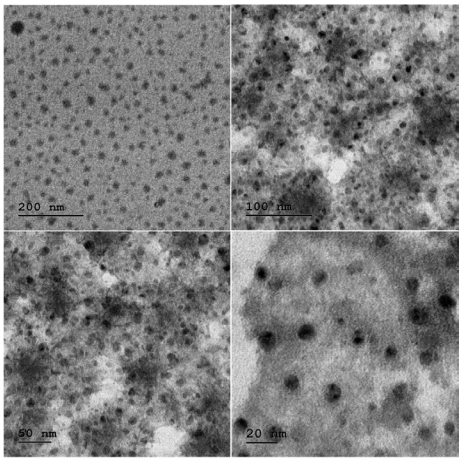

Fig. 6: TEM of optimized batch of FST cubosomes

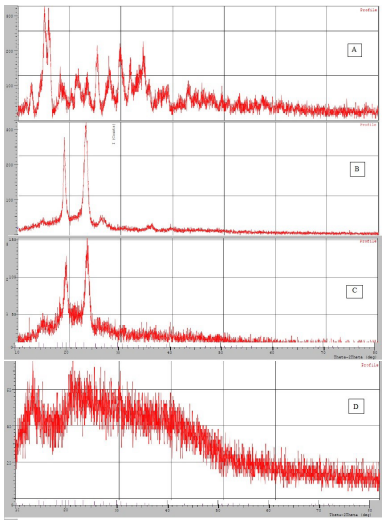

Fig. 7: XRD, (A): FST; (B): GMO; (C): P-407 and (D): FST cubosomes

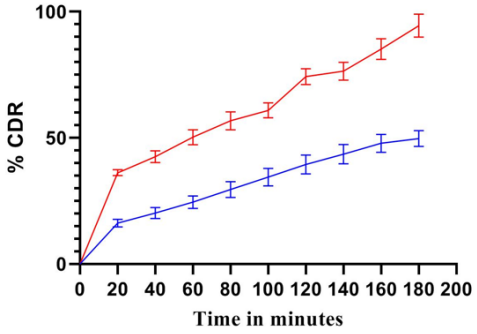

Fig. 8: % CDR *vs.* time of FST cubosomes
Note: (▬): Pure drug and (▬): Optimized FST cubosomes

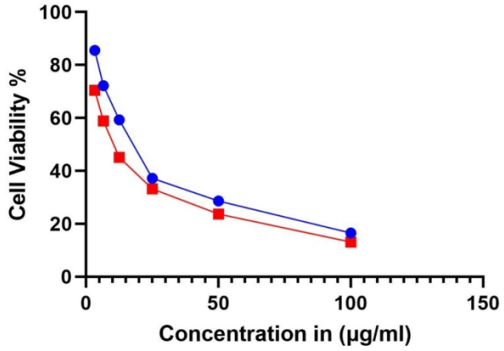

Fig. 9: % Cell viability of plain FST and optimized FST cubosomes
Note: (●): FST and (■): FST cubosomes

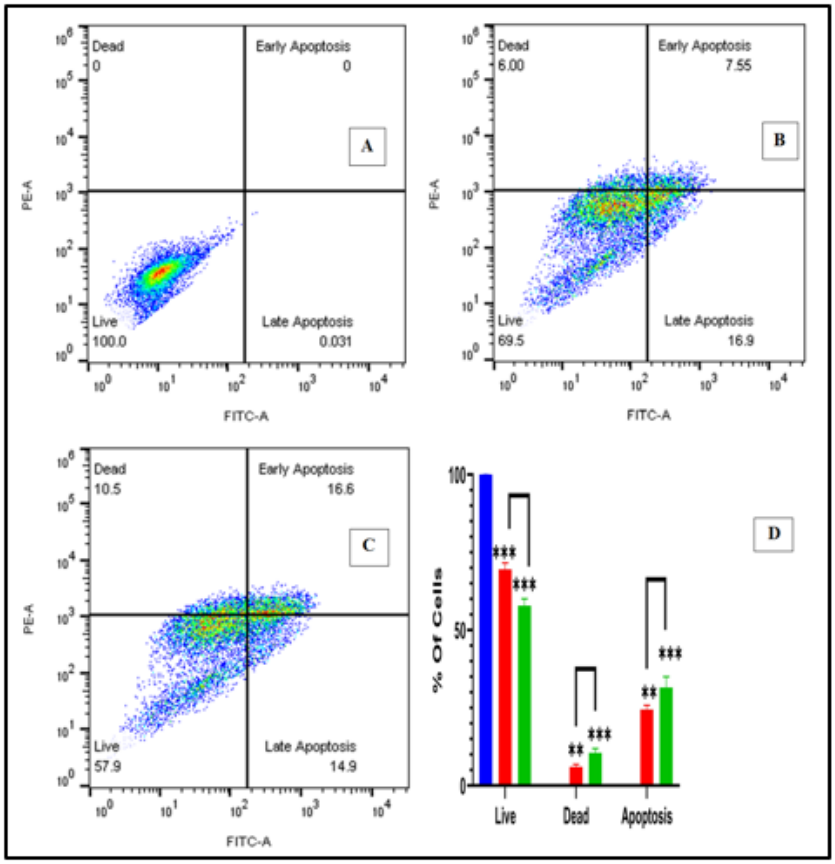

Fig. 10: Flow cytometry, (A): Normal control; (B): FST; (C): Optimized FST cubosomes and (D): Percentage of cells undergoing apoptosis and necrosis compared to control on treatment with FST and FST cubosomes for 12 h
Note: (■): Control; (■): FST and (■): FST-cubosomes

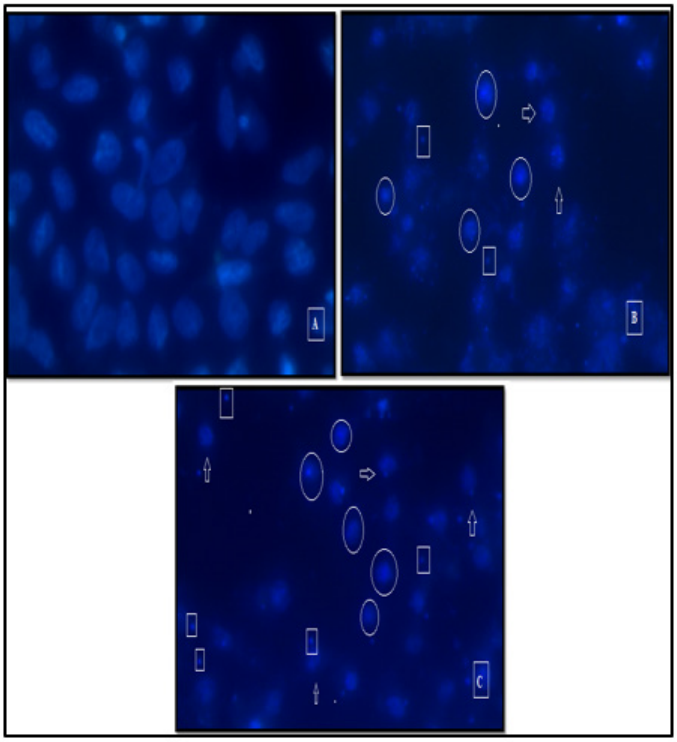

Fig. 11: DAPI apotosis, (A): Normal control; (B): FST and (C): Optimized FST cubosomes

Cell morphology was used to study anticancer-potential of FST cubosomes by evaluating morphological changes. LNCaP cells on treatment with plain FST and lyophilized FST cubosomes for 48 h are shown in fig. 12. In the control group, the cells observed were spindle-shaped and showing higher confluency of monolayer cells (fig. 12A). In contrast, LNCaP cells treated with plain FST (fig. 12B), and lyophilized FST cubosomes (fig. 12C), lost their normal morphology, shrank, detached and showed a more significant reduction in the number.

The % EE of optimized FST cubosomes was found to be (fresh-93.06 %±0.04 %, 1 mo-92.74 %±0.58 %, 2 mo-92.58 %±0.55 % and 3 mo-92.37 %±0.42 %) respectively while the % FST release was observed to be (fresh-93.68 %±3.67 %, 1 mo-93.41 %±3.23 %, 2 mo-93.21 %±2.98 % and 3 mo-93.15 %±2.73 %) respectively after 3 h. Thus, the obtained results clearly revealed high stability of cubosomes at 40°±2°/75 %±5 % RH.

The FTIR and DSC analysis conformed the compatibility of FST to cubosomal excipients. The fundamental peaks of the FST are retained in the formulation indicating no chemical interaction between FST and excipients used[26]. Besides DSC studies revealed that FST incorporated in the cubosomes is existed in amorphous state indicating that FST might be molecularly dispersed in cubosomal vesicles. The % EE of cubosomes was found to be dependent on the concentration of GMO. The augment in % EE was observed with an increase in the concentration of GMO. Furthermore, the vesicle size has unique value in vesicular drug delivery system. Vesicle size of developed FST cubosomes was found in nanosize which is the best fitted for the vesicular delivery[24]. Vesicle size of cubosomal dispersions primly depends on concentration of GMO with GMO/P-407 ratio. At low GMO concentration, a small vesicle size was obtained and vice versa[27-29]. The high ZP value of FST-loaded cubosomes indicates better stability of developed system. This high value may be attributed to the presence and concentration of P-407/ GMO in the cubosomes[30]. Moreover, P-407 may play a crucial role in the negative ZP value of cubosomal vesicles as P-407 induces a transition in the charge of the vesicles from positive to negative. Also there is a strong possibility of hydrogen bonding among the hydroxyl groups in the P-407 which decreases vesicles size as the concentration of P-407 increases[31,32]. The surface morphology of optimized FST cubosomes confirmed that cubosomes are cubical in shape having smooth appearance which is confirmed by TEM results. The XRD study results of FST-loaded cubosomes indicate that the FST might be molecularly dispersed in non-crystalline state or changed to amorphous state[33]. *In vitro* release of FST from lyophilized FST cubosomes

was found to be substantially higher than plain FST solution. This higher release of FST from the lyophilized FST cubosomes could be due to the decrease in the vesicle size. Moreover, the FST cubosomes exhibited momentous *in vitro* cytotoxicity towards LNCaP cells than plain FST. Thus, remarkably increased cytotoxicity of cubosomes against prostate cancer might be due to enhanced intracellular uptake and endocytosis of FST cubosomes[34,35]. Moreover, the nanovesicle size range and rapid release of FST from cubosomes also responsible for higher cytotoxicity. In tumor, apoptosis is the key mechanism by which anticancer moiety can induce cell death. The cells treated with FST cubosomes showed reduction in live cells, and increased % of apoptotic cells revealing high efficacy and quick uptake of FST loaded cubosomes by cancerous cells[36]. Moreover, apoptotic potential of FST cubosomes was investigated against LNCaP cells using the Annexin V-FITC/PI staining technique. Apoptotic potential always accompanied with movement of phosphatidyl serine from cytosol to cell membrane. Results of flow-cytometry displayed a great extent of cells entered in apoptotic stage when treated with FST cubosomes as compared to control. Evaluation of nuclear morphology by fluorescence microscopy using a DAPI stain is commonly used for apoptosis analysis. Apoptosis by DAPI indicate that FST cubosomes induce apoptosis in LNCaP cells crumbling of nuclei and irregular edges close to the nuclei which are a sign of cell undergoing apoptosis. In normal control cells, unharmed nucleus was observed whereas in FST cubosomes treated cells nuclear condensation and nuclear breakup of cells was observed[37]. This type of morphological alterations reveals cell apoptosis subsequent the treatment with FST cubosomes indicating their powerful cytotoxic activity. Furthermore, no significant alterations were observed in the drug content and cumulative % FST release after 3 mo storage of optimized cubosomes at 40±2°/75 %±5 % RH indicating its better stability.

In summary, FST-cubosomes using GMO and P407 was successfully developed through optimization by the Box-Behnken statistical design. The optimized vesicles were cubic in shape with an EE of 92.54±2.67 %. The vesicular delivery approach might increase the cellular uptake of FST; overall, the cubosomal formulation approach for the FST could be used as an effective delivery tool for improved efficacy against prostate cancer cells; however, further studies are recommended to explore and establish the safety and efficacy in *in vivo* models.

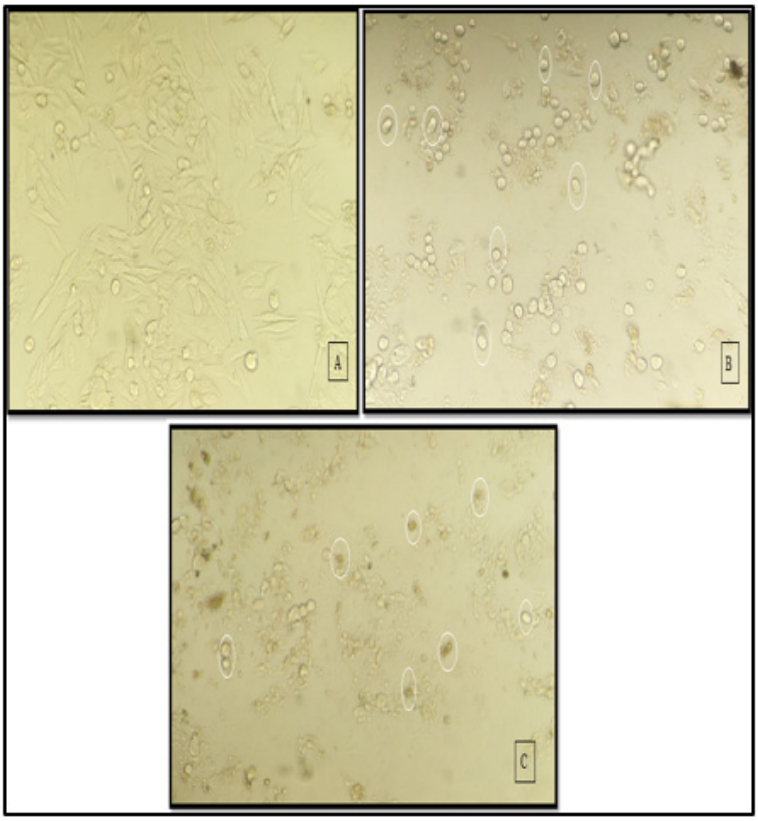

Fig. 12: Cell morphology, (A): Normal control; (B): FST and (C): Optimized FST cubosomes

Acknowledgements:

The authors would like to express their gratitude to the Department of Pharmacy, Sant Gajanan Maharaj College of Pharmacy, Mahagaon, and the Trustees of Sant Gajanan Maharaj College of Pharmacy, Mahagaon, for their guidance and support in completing this research. The authors also thank Maratha Mandal Dental College and Research Center, Belagavi, for conducting the anticancer activity studies, Diaya Labs, Mumbai, and the Department of Science and Technology-Sophisticated Analytical Instrumentation Facility (DST-SAIF), Cochin, for their assistance with the analytical work.

Conflict of interest:

The authors declared there is no conflict of interests.

REFERENCES

1. Ng CY, Yen H, Hsiao HY, Su SC. Phytochemicals in skin cancer prevention and treatment: An updated review. Int J Mol Sci 2018;19(4):941.
2. Mazhar D, Waxman J. Prostate cancer: Review. Postgr Med J 2002;78(924):590-5.
3. Rao SV, Sravya BN, Padmalatha K. A review on cubosome: The novel drug delivery system. GSC Biol Pharm Sci 2018;5(1):76-81.
4. Bhosale RR, Osmani RA, Harkare BR, Ghodake PP. Cubosomes: The inimitable nanoparticulate drug carriers. Scholars Acad J Pharm 2013;2(6):481-6.
5. Fahmy UA, Fahmy O, Alhakamy NA. Optimized icariin cubosomes exhibit augmented cytotoxicity against SKOV-3 ovarian cancer cells. Pharmaceutics 2020;13(1):1-21.
6. Hamedi S, Shojaosadati SA. Rapid and green synthesis of silver nanoparticles using *Diospyros lotus* extract: Evaluation of their biological and catalytic activities. Polyhedron 2019;171:172-80.
7. Ahmed S, Ahmad M, Swami BL, Ikram S. Green synthesis of silver nanoparticles using *Azadirachta indica* aqueous leaf extract. J Radiation Res Appl Sci 2016;9(1):1-7.
8. Nasr M, Ghorab MK, Abdelazem A. *In vitro* and *in vivo* evaluation of cubosomes containing 5-fluorouracil for liver targeting. Acta Pharm Sin B 2015;5(1):79-88.
9. Nasr M, Younes H, Abdel-Rashid RS. Formulation and evaluation of cubosomes containing colchicine for transdermal delivery. Drug Deliv Transl Res 2020;10(5):1302-13.
10. Galatage ST, Parpolkar DS. Design and characterization of silver nanoparticles of *Momordica charantinai* Linn. by green synthesis. IJPSR 2020;11(4):1808-15.
11. Hundekar YR, Saboji JK, Patil SM, Nanjwade BK. Preparation and evaluation of diclofenac sodium cubosomes for percutaneous administration. World J Pharm Pharm Sci 2014;3(5):523-39.
12. Killedar SG, Bhagwat DA, Choudhari A, Saboji JK, Chougule PC, Galatage ST. Development and characterization of microsponge of amphotercin B for topical drug delivery. Res J Pharm Biol Chem Sci 2019;10(1):1288-300.
13. Teagarden DL, Anderson BD, Petre WJ. Determination of the pH-dependent phase distribution of prostaglandin El in a lipid emulsion by ultrafiltration. Pharm Res 1988;5:482-7.
14. Gupta PK, Hung CT, Perrier DG. Quantitation of the release of doxorubicin from colloidal dosage forms using dynamic dialysis. J Pharm Sci 1987;76(2):141-5.
15. Namdeo A, Jain NK. Niosomal delivery of 5-fluorouracil. J Microencapsul 1999;16(6):731-40.
16. Mosmann T. Rapid colorimetric assay for cellular growth and survival: Application to proliferation and cytotoxicity assays. J Immunol Methods 1983;65(1-2):55-63.
17. Kumbar VM, Peram MR, Kugaji MS, Shah T, Patil SP, Muddapur UM, *et al*. Effect of curcumin on growth, biofilm formation and virulence factor gene expression of *Porphyromonas gingivalis*. Odontology 2021;109(1):18-28.
18. Galatage ST, Hebalkar AS, Gote RV, Mali OR, Killedar SG, Bhagwat DA, *et al*. Design and characterization of camptothecin gel for treatment of epidermoid carcinoma. Future J Pharm Sci 2020;6:1.
19. Peram MR, Jalalpure S, Kumbar V, Patil S, Joshi S, Bhat K, *et al*. Factorial design based curcumin ethosomal nanocarriers for the skin cancer delivery: *In vitro* evaluation. J Liposome Res 2019;29(3):291-311.
20. Bhat SS, Revankar VK, Kumbar V, Bhat K, Kawade VA. Synthesis, crystal structure and biological properties of a cis-dichloridobis (diimine) copper (II) complex. Acta Crystallogr Section C Struct Chem 2018;74(2):146-51.
21. Newa M, Bhandari KH, Oh DH, Kim YR, Sung JH, Kim JO, *et al*. Enhanced dissolution of ibuprofen using solid dispersion with poloxamer 407. Arch Pharm Res 2008;31:1497-507.
22. Han L, Wang T. Preparation of glycerol monostearate from glycerol carbonate and stearic acid. RSC Adv 2016;6(41):34137-45.
23. Jia P, Bo C, Hu L, Zhou Y. Synthesis and characterization of glyceryl monooleate-based polyester. Korean J Chem Eng 2015;32:547-51.
24. Danaei MR, Dehghankhold M, Ataei S, Hasanzadeh Davarani F, Javanmard R, Dokhani A, *et al*. Impact of particle size and polydispersity index on the clinical applications of lipidic nanocarrier systems. Pharmaceutics 2018;10(2):57.
25. Honary S, Zahir F. Effect of zeta potential on the properties of nano-drug delivery systems-A review (Part 2). Trop J Pharm Res 2013;12(2):265-73.
26. Veras KS, Fachel FN, Pittol V, Garcia KR, Bassani VL, Dos V, *et al*. Compatibility study of rosmarinic acid with excipients used in pharmaceutical solid dosage forms using thermal and non-thermal techniques. Saudi Pharm J 2019;27(8):1138-45.
27. Badran M. Formulation and *in vitro* evaluation of flufenamic acid loaded deformable liposomes for improved skin delivery. Digest J Nanomater Biostruct 2014;9(1):83-91.
28. Chen M, Liu X, Fahr A. Skin penetration and deposition of carboxyfluorescein and temoporfin from different lipid vesicular systems: *In vitro* study with finite and infinite dosage application. Int J Pharm 2011;408(1-2):223-34.
29. Clogston JD, Patri AK. Zeta potential measurement. Methods Mol Biol 2011:697:63-70.
30. Putri DC, Dwiastuti R, Marchaban AK. Optimization of mixing temperature and sonication duration in liposome preparation. J Pharm Sci Commun 2017;14(2):79-85.
31. Hao Y, Zhao F, Li N, Yang Y. Studies on a high encapsulation

of colchicine by a niosome system. Int J Pharm 2002;244(1-2):73-80.
32. Barauskas J, Johnsson M, Tiberg F. Self-assembled lipid superstructures: Beyond vesicles and liposomes. Nano Lett 2005;5(8):1615-9.
33. Alwadei M, Kazi M, Alanazi FK. Novel oral dosage regimen based on self-nanoemulsifying drug delivery systems for codelivery of phytochemicals-curcumin and thymoquinone. Saudi Pharm J 2019;27(6):866-76.
34. Galatage ST, Trivedi R, Bhagwat DA. Characterization of camptothecin by analytical methods and determination of anticancer potential against prostate cancer. Future J Pharm Sci 2021;7(1):104.
35. Zhang YP, Li YQ, Lv YT, Wang JM. Effect of curcumin on the proliferation, apoptosis, migration, and invasion of human melanoma A375 cells. Genet Mol Res 2015;14(1):1056-67.
36. Bhagwat DA, Swami PA, Nadaf SJ, Choudhari PB, Kumbar VM, More HN, *et al*. Capsaicin loaded solid SNEDDS for enhanced bioavailability and anticancer activity: *In vitro*, *in silico*, and *in vivo* characterization. J Pharm Sci 2021;110(1):280-91.
37. Yallapu MM, Othman SF, Curtis ET, Bauer NA, Chauhan N, Kumar D, *et al*. Curcumin-loaded magnetic nanoparticles for breast cancer therapeutics and imaging applications. Int J Nanomed 2012:1761-79.